Progress In Electromagnetics Research Letters, Vol. 102, 87–94, 2022

Near-Field Measurement System Based on a Software Defined Radio

Marcelo B. Perotoni[*] [1], Leandro A. Silva[1], Walter Silva[1], and Kenedy M. G. Santos[2]

Abstract—This article reports an SDR (software-defined radio) operating as a receiver for near-field measurement, aiming at EMC pre-compliance tests. The SDR replaces professional-grade RF instrumentation with benefits, with lower costs. Its software application is based on open-source GNU-Radio, which grants a higher versatility to the signal processing and visualization, requiring a single laptop to analyze the data and control the whole system, in real time. Reported tests used two commercial PCB magnetic field probes, and a proof-of-concept near-field imaging is performed in an L-shaped transmission line at 1100 MHz.

1. INTRODUCTION

Pre-compliance, though not exactly defined [1] within EMC, encompasses practices and measurements that are not performed using accredited installations or laboratories, nevertheless help finding and correcting possible problems whose later fixes might become too expensive or time-consuming [2]. Complementary to electromagnetic simulation tools, low-cost EMC instrumentation can not only help the identification of possible problems but also grant insight into common pitfalls, shortening design cycles.

For pre-compliance, near-field probes (NFPs) are well-known instruments used for Electric and Magnetic Fields [3]. NFPs connected to oscilloscopes or spectrum analyzers allow the investigation of hot spots in PCBs, harnesses, or complex environments, where full-wave simulation is not feasible. They can spatially locate emission sources inside an instrument or system [4], and some commercial scanners contain arrays of small loops performing computer-controlled measurements in PCBs [5]. Transitory signals can be captured in real time using oscilloscopes [6], and by monitoring the frequency content of the radiated signal it is possible to visualize emissions of higher-order harmonics, multiple of clock signals in digital boards, which might radiate efficiently due to the associated circuit layout [7]. Information on the near field also allows replacing the actual structure by equivalent radiating sources (dipoles or loops), which simplifies further analyses and implementation of efficient virtual studies [8, 9].

This article describes an SDR connected to a set of NFPs that make up an affordable, versatile, and ligh weight system to be used in pre-compliance activities. A GNU Radio application interfaces with the SDR, a tool that contains several signal-processing functions organized in a free yet powerful block-oriented suite. Filtering, decimation, time-analyses, and other functions can be implemented using GNU Radio in an intuitive and rapid way. Fig. 1 shows the basic idea. The direct SDR connection to a laptop enables a versatile and light weight application since there is no need for AC connection; the SDR is powered up directly by the USB connection. Complex analysis and visualization of the SDR-incoming data can be performed real time. Device sensitivity, probe calibration, and software application are discussed and finalized with the fields captured from a test PCB, at 1100 MHz.

Received 11 November 2021, Accepted 17 December 2021, Scheduled 19 January 2022
* Corresponding author: Marcelo Bender Perotoni (mperoconsult@gmail.com).
[1] UFABC, Brazil. [2] IFBA, Brazil.

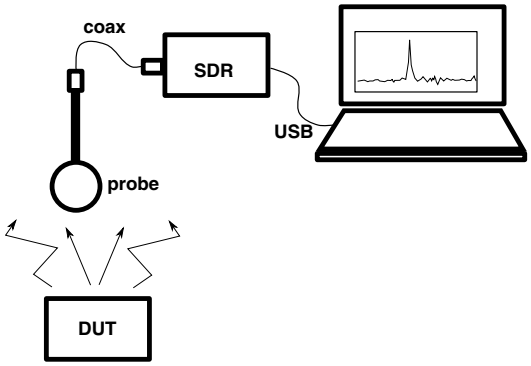

Figure 1. Block diagram of the proposed NF measurement system based on a SDR.

2. SDR AND GNU RADIO

HackRF One is an open-source SDR project, covering the range of 10 MHz to 6 GHz, based on an 8-bits ADC (analog-to-digital converter). It has an internal 14 dB LNA, switchable by software. Its single RF channel can be set as either transmitter or receiver (half-duplex). It has been used in several different applications, such as RF exposure assessment [10], as a testbed for avionic wireless tests [11], as an education tool [12] and to measure WiFi spectrum occupancy [13]. SDR sensitivity is primarily defined by the the number of bits of its ADC. A first-order SNR (signal-to-noise ratio) estimate for an ADC with N bits can be written as [14]:

$$\text{SNR} = 6.02N + 1.76 \tag{1}$$

The more realistic parameter $ENOB$ expresses the ADC effective number of bits, since it considers other factors besides the mathematical conversion of an analog signal subjected to quantization noise. For instance, high-amplitude carriers can saturate the RF circuits and generate intermodulation products; therefore, they define maximum allowed input amplitudes. In the particular case of HackRF One and similar commercial SDRs, FM broadcast carriers in urban environment are usually mainly responsible for this upper bound, due to their high amplitudes.

A comparison between the noise floor figures (NoFl) of a spectrum analyzer (SA) (Rohde & Schwarz FS315) and the SDR is performed, and the results are shown in Fig. 2. The SA has, besides its default operation, a "High Sensitivity" mode. The SDR was connected to an RF generator, whose output power was set to 10 dB above the noise level measured on the GNU Radio application, thereby allowing

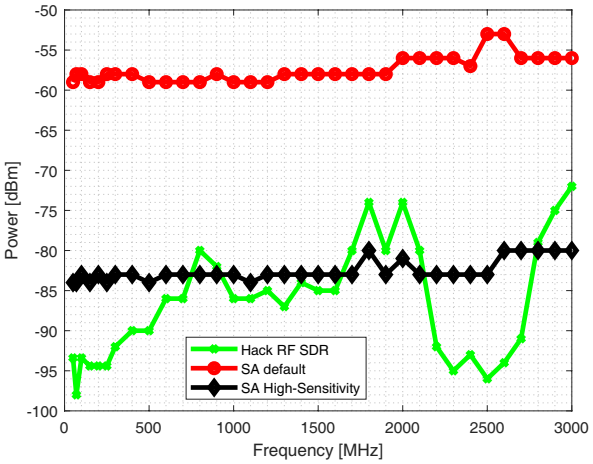

Figure 2. Comparison of the sensitivity (NoFl) of the HackRF One SDR with a commercial SA, the latter operating in default and high-sensitivity.

the NoFl to be determined by subtracting this 10 dB from the generator output power setting. Both devices were set with the same 20-MHz bandwidth, with average and LNA switched off in the SDR.

Results show that the SDR has similar sensitivity to the SA High-Sensitivity operation. A peculiar optimal point of the SDR sensitivity is found around 2500 MHz, probably due to SDR chipsets originally optimized for this unlicensed ISM (Industrial, Scientific and Medical) range. Sensitivity can be artificially improved with software techniques, commonly used together, such as averaging, oversampling, or decimation.

SDRs interface with several different software suites, among them GNU Radio. GNU Radio Companion offers the possibility of generating a complete signal processing analysis using the SDR incoming samples in a block-diagram design environment, similar to LabView. The final program can be deployed independently of GNU Radio by means of a Python script. Once the samples are captured by a block named osmocom, they circulate in a time-domain stream among the different blocks. Frequency domain is displayed using visualization tools, using the dBr (relative dB) unit, which requires a calibration to convert to dBm.

The used flowgraph (Fig. 3) contains a block that displays the spectral representation of the incoming signal (QT GUI Frequency Sink), however without access to the FFT data samples. For that matter, an FFT block was used. A number sink block retains the peak value of the computed frequency domain operation, shown in a label for easy reading during the actual measurement procedure. Additional blocks implement the necessary corrections for showing the power in dBm.

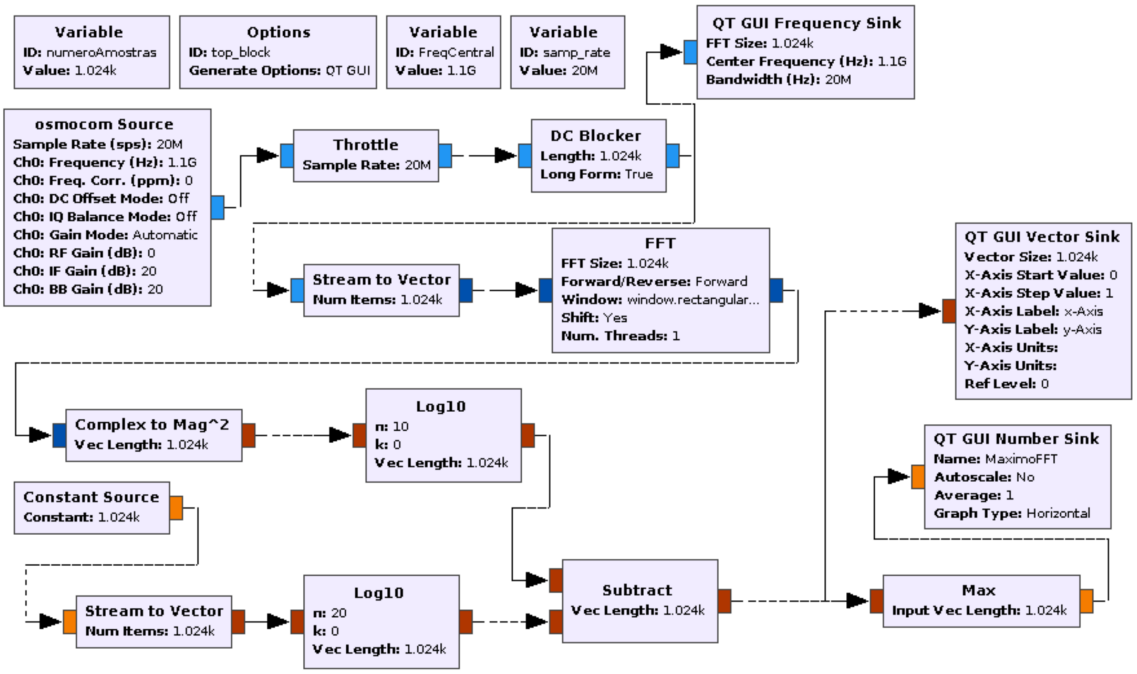

Figure 3. GNU Radio program containing the FFT of the incoming signal and routines to fetch its peak across the band, along unit conversion to dBm.

3. PROBES AND CHARACTERIZATION

Magnetic NFPs are in general designed using electrically small loops, whereas electric cones are based on monopole-like structures [3, 15]. They can be improvised using short sections of coaxial cables or PCBs [16, 17]. For the sake of pre-compliance, there might be enough finding peak resonances in normalized field measurements; however if there is a need to estimate the absolute field value, a calibration is needed. In short, the relation between probe power and voltage can be related to the sampled field

amplitude by means of the Antenna Factor (AF) parameter:

$$AF_H = \frac{H}{P_{out}} \tag{2}$$

$$AF_E = \frac{E}{P_{out}} \tag{3}$$

where AF_H and AF_E are respectively magnetic (H) and electric (E) Antenna Factors. P_{out} represents the probe output power in response to the existing field, and in the case of an oscilloscope the time-domain voltage is used instead. Some options to determine field amplitudes to compute the AF:

- Comparison with similar calibrated probes.
- GTEM (Gigahertz Transverse-Electromagnetic) cells have an internal volume where absolute field values are known, so the correlation with probes output power or voltages is direct [18].
- In regard to AF_H, for lower frequencies where impedance mismatches effects are not relevant, a loop (radius R) is excited by a generator in series with a resistor [19]. Voltage drop across the resistor, measured in an oscilloscope, informs the exciter current I_E; therefore, the magnetic field H at a distance y along the loop axis can be analytically found after Ampère law:

$$H(y) = \frac{I}{2\pi\left[y^2 + R^2\right]^{3/2}} \tag{4}$$

- Use of a TEM structure whose fields can be either analytically described or found after numerical simulations [20].

For this work, a calibration procedure used a planar TEM structure is shown in Fig. 4 with the respective dimensions. Its termination is made by two parallel-SMD 100 Ω resistors, and the generator connects to a common low-cost SMA-type coaxial SMA. To check out the virtual simulation consistency, FEKO and CST evaluations were performed; the former based on MoM (Method of Moments) and the latter using FIT (Finite Integration Technique). Since there were no calibrated probes available, the reflection impedance (S_{11} parameter) was used as comparison among the two simulation results and the measurement, covering the range of 10 MHz to 3 GHz, and results are also shown in Fig. 4.

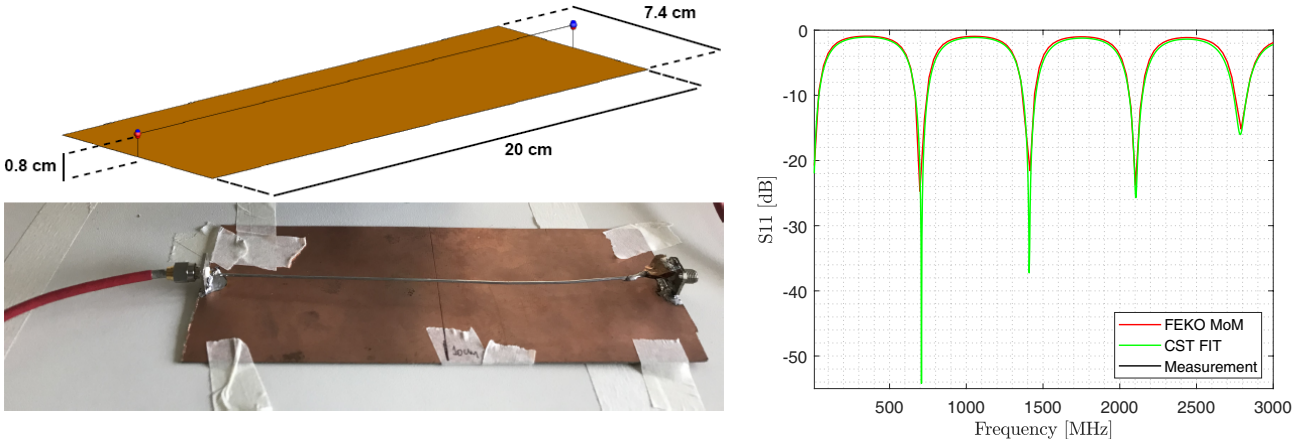

Figure 4. Test circuit and comparison of the measured and computed S_{11} at its input port.

S_{11} results present a good correlation between measurement and simulations, pointing a consistency in the virtual model. Next, the fields are recorded in the FEKO model at 1 cm above the middle point of the transmission line, mimicking the measurement. Field amplitudes in the simulation were duly scaled-up to comply with the generator 17 dBm excitation power. A house-made, three-axis XYZ matrix is used to guarantee the mechanical precision, shown in Fig. 5. Its 1-mm resolution in the three axes is achieved by means of stepper motors and associated gear. Its control is performed by a Labview application, with an Arduino board interfacing with three motor drivers.

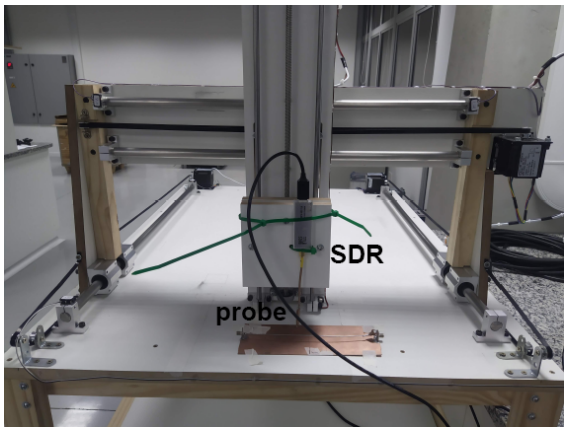

Figure 5. Test-board positioned on the XYZ matrix. An SDR is seen connected to a magnetic NFP over the board.

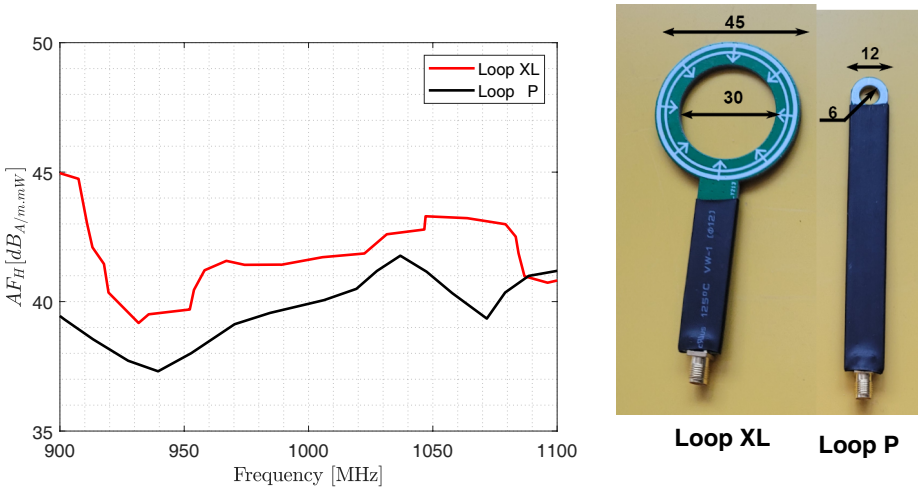

Figure 6. AF_H for two different sizes NFP, along with their diameter dimensions [mm].

Two different planar magnetic NFPs have their AF_H shown in Fig. 6, evaluated from 900 MHz to 1100 MHz. It can be seen that the physically larger loop (XL) has better sensitivity, at expenses of a poorer spatial resolution when being used for imaging. Since decibel units are used for the measurement, conversion from dBm readings to the field amplitudes (e.g., dBA/m) can be found after:

$$H = AF_H + P_{out} \tag{5}$$

with all variables expressed in decibels.

4. IMAGING APPLICATION

A test board was designed to be imaged using the XYZ matrix and the HackRF One connected to a magnetic NFP. Since field imaging is the point of interest, a small ("P") loop probe was chosen (Fig. 7). The probe was positioned 2 cm above the ground plane, and the wire on the board was shaped with a 90° angle to make it more visible. Preliminary tests showed that the probe proximity to the moving head (wood with metallic bolts) distorted the fields, so a plastic container was positioned as a way to keep probe and matrix head physically separated.

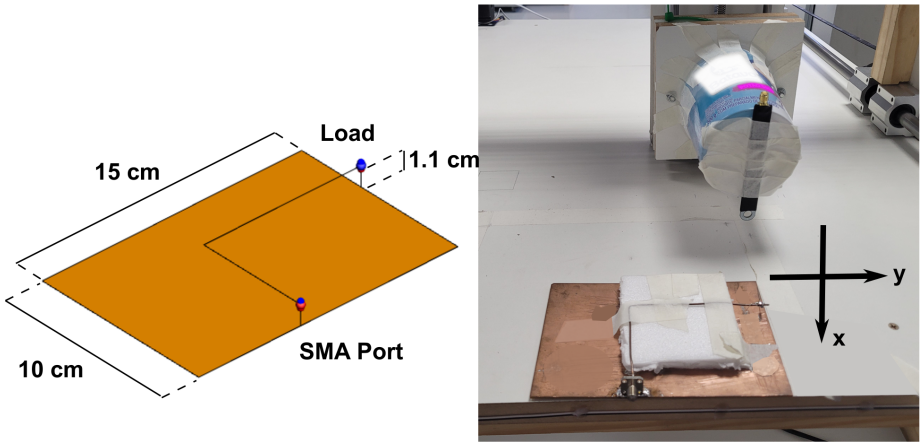

(a) (b)

Figure 7. (a) Test board to be imaged, dimensions [cm]. (b) Actual measurement setup, the Styrofoam layers were used as a spacer in the board.

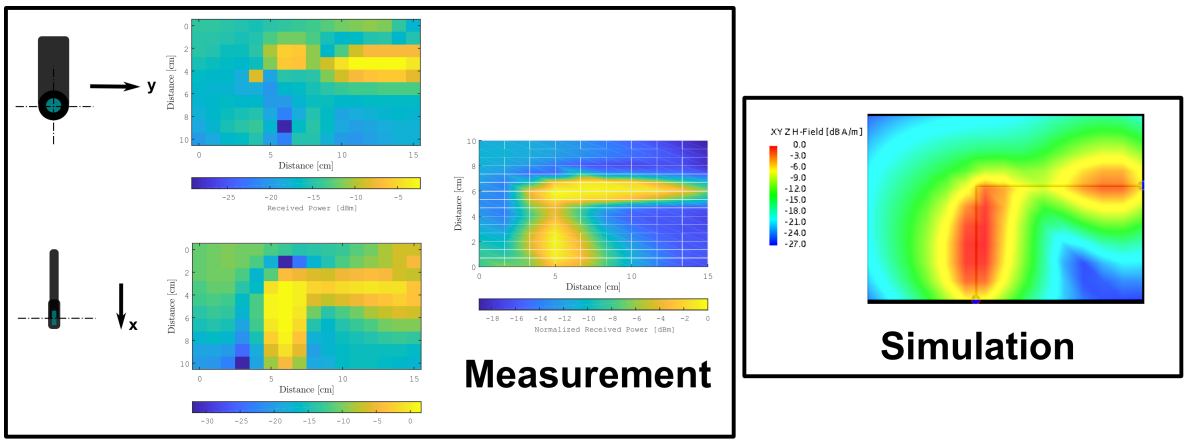

Figure 8. Results of the Near-field scanning with the magnetic loop. Left box, measurements: left, sweeping with two different probe orientations and right, results of the combined orthogonal magnitudes. Right box, FEKO simulation.

The imaging process swept the board in a 1-cm square grid, using Labview to command the moving head and the GNU Radio application (Fig. 3) to read the maximum output power across the 20 MHz bandwidth. The test board was fed with 15 dBm, 1100 MHz continuous wave. Fig. 8 contains the NF readings for the probes oriented according to the x and y axes, alongside the absolute field value obtained after combination of the former magnitudes, normalized and enhanced with a post-processing interpolation routine. A FEKO simulation containing the same 1-cm grid is also presented for comparison.

From the results it is possible that in spite of the rough 1-cm resolution scanning grid (which took 30 minutes for each scan), a clear image is obtained. A particular pixel with error (top left, close to $x = 5$ and $y = 4$) can be eliminated by averaging the measurement and/or finer mesh, at the expense of a longer acquisition. Dynamic range of the measurement data was 19 dB, a parameter that impacts the resolution since low amplitudes might be below the Noise Floor. The maximum received input power was 2 dBm, so care should be taken in order not to overload the SDR RF frontend. A more complex PCB might need the SDR LNAs switched on, or even the use of additional external LNAs in order

to bring the picked up power into the SDR usable dynamic range. That versatility of the hardware modification and post-processing functions contrast the SDR use with that from an ordinary spectrum analyzer.

5. CONCLUSIONS

Integration of an SDR into a near-field measurement system is presented, using a pair of magnetic probes calibrated with help of numerical simulation. The system, with the help of a 3-axes positioning matrix, imaged an L-shaped TEM line board, using GNU Radio as software interface with the SDR. It has lower costs (USD 390 for the SDR) and higher versatility than solutions based on professional instrumentation (spectrum analyzers or oscilloscopes), and it is light weight and does not need AC connection to be powered up. For the sake of application, GNU Radio affords a free yet much lighter and powerful way to filter and process the incoming data, in real time, unlikely to be surpassed by commercial RF instruments.

REFERENCES

1. Videnka, R. and J. Svacina, "Introduction to EMC pre-compliance testing," *MIKON 2008 — 17th International Conference on Microwaves, Radar and Wireless Communications*, 1–4, 2008.
2. Schneider, D., S. Tenbohlen, and W. Köhler, "Pre-compliance test method for radiated emissions of automotive components using scattering parameter transfer functions," *International Symposium on Electromagnetic Compatibility — EMC EUROPE*, 1–6, 2012.
3. Bienkowski, P. and H. Trzaska, *Electromagnetic Measurements in the Near-field*, Scitech, Raleigh, 2012.
4. Baudry, D., F. Bicrel, L. Bouchelouk, A. Louis, B. Mazari, and P. Eudeline, "Near-field techniques for detecting EMI sources," *2004 International Symposium on Electromagnetic Compatibility*, 11–13, 2004.
5. Montrose, M. I. and E. M. Nakauchi, *Testing for EMC Compliance: Approaches and Techniques*, IEEE Press, Piscataway, 2004.
6. Kuznetsov, Y., A. Baev, A. Gorbunova, M. Knovalyuk, D. Thomas, C. Smartt, M. H. Baharuddin, J. A. Russer, and P. Russer, "Localization of the equivalent sources on the PCB surface by using ultra-wideband time domain near-field measurements," *International Symposium on Electromagnetic Compatibility — EMC EUROPE*, 1–6, 2016.
7. Kuznetsov, Y., A. Baev, M. Konovalyuk, A. Gorbunova, M. Haider, J. A. Russer, and P. Russer, "Characterization of the cyclostationary emissions in the near-field of electronic device," *International Symposium on Electromagnetic Compatibility — EMC EUROPE*, 573–578, 2018.
8. Ramesan, R. and D. Madathil, "Modeling of radiation source using an equivalent dipole moment model," *Progress In Electromagnetics Research B*, Vol. 89, 157–175, 2020.
9. Foged, L. J., L. Scialacqua, F. Saccardi, F. Mioc, M. Sørensen, G. Vecchi, and J. L. A. Quijano, "Using measured fields as field sources in computational EMC," *37th Annual Symposium of the Antenna Measurement Techniques Association, AMTA*, 223–227, 2015.
10. Bechet, A. C., C. Helbet, I. Bouleanu, A. Sarbu, S. Miclaus, and P. Bechet, "Low cost solution based on software defined radio for the RF exposure assessment: A performance analysis," *11th International Symposium on Advanced Topics in Electrical Engineering (ATEE)*, 1–6, 2019.
11. Sommer, D., A. S. C. R. Irigireddy, J. Parkhurst, and E. R. Nastrucci, "SDR- and UAV-based wireless avionics intra-communication testbed," *AIAA/IEEE 39th Digital Avionics Systems Conference (DASC)*, 1–5, 2020.
12. Del Barrio, A. A., J. P. Manzano, V. M. Maroto, A. Villarin, J. Pagan, M. Zapater, J. Ayala, and R. Hermida, "Hack-RF + GNU radio: A software-defined radio to teach communication theory," *International Journal of Electrical Engineering & Education*, 1–18, 2019.

13. Pacurar, O. T., C. Balint, C. Iftode, A. M. Silaghi, and A. D. Sabata, "Spectrum occupancy measurements in the Wi-Fi band with a PCB antenna," *International Symposium on Electronics and Telecommunications (ISETC)*, 1–4, 2020.
14. Collins, T. F., R. Getz, D. Pu, and A. M. Wyglinski, *Software-defined Radio for Engineers*, Artech House, Norwood, 2018.
15. Baudry, D., A. Louis, and B. Mazari, "Characterization of the open-ended coaxial probe used for near-field measurements in EMC applications," *Progress In Electromagnetics Research*, Vol. 60, 311–333, 2006.
16. Sivaraman, N., F. Ndagljlmana, M. Kadi, and Z. Riah, "Broad band PCB probes for near field measurements," *International Symposium on Electromagnetic Compatibility — EMC EUROPE*, 1–5, 2017.
17. Martinez, P. A., E. A. Navarro, J. Victoria, A. Suarez, J. Torres, A. Alcarria, J. Perez, A. Amaro, A. Menendez, and J. Soret, "Design and study of a wide-band printed circuit board near-field probe," *Electronics*, Vol. 10, No. 18, 1–19, 2021.
18. Wu, I., S. Ishigami, K. Gotoh, and Y. Matsumoto, "Probe calibration by using a different type of probe as a reference in GTEM cell above 1 GHz," *IEICE Electronics Express*, Vol. 7, No. 6, 460–466, 2010.
19. Fano, W. G., R. Alonso, and L. M. Carducci, "Near field magnetic probe applied to switching power supply," *2016 IEEE Global Electromagnetic Compatibility Conference (GEMCCON)*, 1–4, November 2016.
20. Dimitrijević, T., A. Atanaskovic, N. Doncŏv, D. Thomas, C. Smartt, and M. Baharuddin, "Calibration of the loop probe for the near-field measurement," *International Journal of Microwave and Wireless Technologies*, Vol. 12, No. 9, 878–884, 2020.